Conformational Changes in a Mammalian Voltage-Dependent Potassium Channel Inactivation Peptide†

Geoffrey W. Abbott,‡,§ Eric A. J. Mercer,‡,|| Rob T. Miller,⊥ Bala Ramesh,‡ and Surjit K. S. Srai*,‡

Department of Biochemistry and Molecular Biology, Royal Free Hospital School of Medicine, Rowland Hill Street, Hampstead, London NW3 2PF, U.K., and Durban Satellite, South African National Bioinformatics Institute, Department of Molecular Virology, University of Natal, Durban, South Africa

Received September 22, 1997; Revised Manuscript Received December 5, 1997

ABSTRACT: Fast inactivation is restored in inactivation deletion mutant voltage-gated potassium (K_V) channels by application of synthetic inactivation 'ball' peptide. Using Fourier transform infrared and circular dichroism spectroscopy, we have investigated the structure of synthetic K_V3.4 channel ball peptide, in a range of environments relevant to the function of the ball domain. The ball peptide contains no α-helix or β-sheet in reducing conditions in aqueous solution, but when cosolubilized with anionic lipid or detergent in order to mimic the environment which the ball domain encounters during channel inactivation, the ball peptide adopts a partial β-sheet structure. Oxidation of the K_V3.4 ball peptide facilitates formation of a disulfide bond between Cys^6 and Cys^{24} and adoption of a partial β-sheet structure in aqueous solution; the tendency of the oxidized ball peptide to adopt β-sheet is generally greater than that of the reduced ball peptide in a given environment. THREADER modeling of the K_V3.4 ball peptide structure predicts a β-hairpin-like conformation which corresponds well to the structure suggested by spectroscopic analysis of the ball peptide in its cyclic arrangement. A V7E mutant K_V3.4 ball peptide analogue of the noninactivating *Shaker* B L7E mutant ball peptide cannot adopt β-structure whatever the environment, and regardless of oxidation state. The results suggest that the K_V3.4 ball domain undergoes a conformational change during channel inactivation and may implicate a novel regulatory role for intramolecular disulfide bond formation in the K_V3.4 ball domain in vivo.

Ion channels are found in most or all eukaryotic cells, mediating ion transport across the cell membrane in order to control membrane potential, secretion, and signal transduction. The complex processing and integration of nervous signals observed in neurons are facilitated by the diverse range of gating properties of the ion channels in this cell type, particularly the voltage-gated potassium (K_V)[1] channels. Fast (N-type) inactivation of K_V channels occurs by a 'ball and chain' mechanism whereby an N-terminal 'ball' domain (inactivation gate) is able to occlude the pore after channel opening to prevent further flow of potassium ions (*1*, *2*). Fast inactivation gives rise to a transient or A-type potassium current, characteristic of *Shaker* channels and certain mammalian homologues. The ball domain is attached to the cytoplasmic side of the channel by an N-terminal chain region and occludes the pore by occupying a site around the inner vestibule of the pore, probably by binding to residues in the S4−5 linker (*3*). Fast inactivation is restored in inactivation deletion mutant channels by application of free synthetic peptide corresponding to the ball domain, indicating that it is the ball region alone which is necessary for fast inactivation (*2*, *3*).

Whereas K_V channel function has been extensively studied using a combination of electrophysiological and molecular biological techniques, the study of K_V channel structure in relation to function is in its infancy. A common feature of K_V channel inactivation ball domains is an N-terminal hydrophobic stretch followed by a region containing a large proportion of polar amino acids, several of which are positively charged. Previous studies have indicated that interaction between the ball domain and its receptor site is facilitated by both electrostatic and hydrophobic interactions (*4*, *5*). Long-range interactions between positive charges on the ball and negative charges on the ball receptor (thought to be within the S4−5 linker) are proposed to initially guide the ball to its inactivation site (*6*, *7*); residues in the hydrophobic stretch of the ball domain then probably bind to a hydrophobic receptor site which only becomes accessible after channel opening, and plug the channel pore (*4*). An additional feature of some K_V channel inactivation ball domains is the presence of cysteine residues which are

† This study was supported by BBSRC (G.W.A.). We gratefully acknowledge the financial support of the Peter Samuel Royal Free Fund.

* Corresponding author. Tel/Fax: 0171 8302453. Email: srai@rfhsm.ac.uk.

‡ Royal Free Hospital School of Medicine.

§ Present address: Department of Cellular and Molecular Physiology, Boyer Center for Molecular Medicine, Yale University School of Medicine, 295 Congress Ave., New Haven, CT.

|| Present address: Department of Developmental Neuroscience, University of Uppsala, Uppsala, Sweden.

⊥ University of Natal.

[1] Abbreviations: CD, circular dichroism; CMC, critical micellization concentration; DTT, dithiothreitol; FTIR, Fourier transform infrared; HPLC, high-pressure liquid chromatography; K_V, voltage-gated potassium; LPC, lysophosphatidylcholine; NMR, nuclear magnetic resonance; PBS, phosphate-buffered saline; PG, phosphatidylglycerol; SDS−PAGE, sodium dodecyl sulfate−polyacrylamide gel electrophoresis; TFA, trifluoroacetic acid; UV, ultraviolet.

S0006-2960(97)02350-7 CCC: $15.00
Published on Web 01/23/1998

implicated in oxidative regulation of channel inactivation (*8*). K_V3.4 channel, found in the mammalian brain, is a fast-inactivating channel incorporating two cysteines in its inactivation ball domain (*8*−*10*). Previous electrophysiological studies have shown that under oxidative conditions the Cys^6 of the K_V3.4 ball domain can be immobilized by formation of a disulfide bond with a cysteine residue on the main body of the channel, and that this prevents N-type channel inactivation (*11*). Furthermore, the two cysteines of the K_V3.4 ball peptide (Cys^6 and Cys^{24}) can be linked to 'cyclise' the peptide in vitro (*12*), but it is not known whether this occurs as a regulatory step in vivo.

The K_V3.4 inactivation ball peptide has recently been shown using NMR spectroscopy to adopt a compact, rigid conformation with no classical secondary structure backbone characteristics in aqueous solution (*13*). In contrast, the mammalian K_V1.4 ball peptide is shown in the same article to contain a stretch of α-helix, and the *Drosophila Shaker* B ball peptide has been previously shown to be unstructured in solution (*4*, *5*). To further investigate the structure of the K_V3.4 inactivation ball in relation to its function, we have used Fourier transform infrared (FTIR) and circular dichroism (CD) spectroscopy to investigate the effect of a range of environments on the structures of 28 residue synthetic peptides corresponding to the K_V3.4 ball domain and to a V7E mutant of the K_V3.4 ball domain, analogous to the noninactivating L7E *Shaker* B mutant ball peptide which cannot facilitate channel inactivation (*4*). FTIR and CD spectroscopy are particularly useful for monitoring secondary structural changes of small peptides in a range of different environments (*14*), especially when using membrane-mimicking lipids and detergents which pose difficulties for other higher-resolution structure determination techniques such as NMR spectroscopy and X-ray crystallography (*15*). Spectroscopic results are compared to structure as predicted by the THREADER modeling program (*16*).

EXPERIMENTAL PROCEDURES

Sample Preparation. K_V3.4 ball peptides (sequence: MISSVC*V*/*E*SSYRGRKSGNKPPSKTCLKEE) were synthesized using a Rainin PS3 automated peptide synthesizer (Protein Technologies, Inc., U.S.A.) by a stepwise solid-phase procedure (*17*) using α-9-fluorenylmethyloxycarbonyl (Fmoc) protecting group strategy (*18*). The peptide was cleaved from the synthesis resin using 95% (v/v) trifluoroacetic acid (TFA) with scavengers and was purified isocratically on a reverse-phase HPLC column (250 × 10 mm internal diameter) using 0.1% (v/v) TFA and acetonitrile as eluents. Following purification, one major peak was observed when the eluent was monitored at 220 nm. The fraction containing pure peptide was lyophilized in the presence of 0.1 M HCl to remove the TFA in preparation for structural studies. To verify purity, ball peptide was checked by amino acid analysis and by mass spectrometry using a Vestec Lasertec Benchtop Laser Desorption Time-of-Flight Mass Spectrometer. Pure K_V3.4 ball peptide was solubilized either in phosphate-buffered saline (pH 7.4) (PBS) made with D_2O for FTIR spectroscopy, or in 100 mM phosphate buffer (pH 7.4) for CD spectroscopy. Reduction of ball peptide was ensured using immobilized dithiothreitol (DTT). Oxidation of ball peptide was achieved by bubbling air through a 10 μM solution of the peptide in $NaHCO_3$ (pH 8.5), with subsequent desalting and lyophilization before solubilization in buffer at pH 7.4. Oxidized ball peptide (wild-type or V7E mutant) gave a single band on an SDS−PAGE gel in the absence of DTT (results not shown) corresponding to the monomeric form of the peptide, indicating that intramolecular rather than intermolecular disulfide bridges were formed by oxidation of the peptide.

Detergent solutions were prepared to either 4 mM or 25 mM concentration in buffer before solubilization of peptide. Lipids, at a lipid:peptide molar ratio of 25:1, were either cosolubilized in lyophilized form with lyophilized peptide in buffer, or buffer-solubilized lipid was added to the buffer-solubilized peptide, with or without vortexing of the sample before or after cosolubilization. Peptide was used at 5−50 mg/mL (FTIR) or 0.4−10 mg/mL (CD). To facilitate direct comparison of different CD spectra, peptide samples were weighed to an accuracy of $\pm<0.01$ mg/mL (1−2% of total sample mass) prior to solubilization so that $\Delta\epsilon$ values could be accurately determined. Neither peptide concentration nor mode of sample preparation affected spectroscopic results.

Infrared Spectroscopy. Samples were loaded into a 10 μL volume gas-tight CaF_2 cell (path length 6 μm). Infrared spectra were recorded using a 1750 Perkin-Elmer FTIR spectrometer continuously purged with dry air. Samples, typically kept at 20 °C, were scanned 100 times and the scans signal-averaged at a resolution of 4 cm^{-1}. For thermal stability measurements, the temperature was varied from 20 to 80 °C with a heating rate of 0.26 °C/min. For each temperature point, 50 scans were signal-averaged at a resolution of 4 cm^{-1}, resulting in measurements every 2 °C. Double-sided interferograms were recorded and apodized using a raised cosine function prior to transformation of the data. The programs IRDM (Perkin-Elmer) and GRAMS (Galactic) were used for data handling. Buffer spectra were recorded under identical conditions to their corresponding protein spectra and subtracted digitally to give a straight base line in the 2100−1800 cm^{-1} area. Deconvolution of spectra was performed using GRAMS Deconvolve (FSD) function. Typically a full width at half-height of 16 cm^{-1} and a Gamma factor of 3.5 were used with 70% Bessel smoothing. Second-derivative spectra were calculated using GRAMS Derivative function with a 13 data point Savitzky−Golay smoothing window.

CD Spectroscopy. Far-UV CD spectra (185−260 nm) were recorded at 20 °C using a Jasco J-600 spectropolarimeter and a range of cell path lengths. The instrument was continuously purged with nitrogen to prevent ozone build-up. Jasco and GRAMS software were used for data handling.

Spectral Assignments. The amide I region (1700−1600 cm^{-1} wavenumbers) of the infrared spectra of proteins is sensitive to protein conformation, and different secondary structure types give rise to characteristic frequencies of absorbance within this region. FTIR amide I absorbance bands were assigned to secondary structures according to Jackson and Mantsch (*19*), after resolution enhancement using second derivation of the absorbance spectra. Three representative secondary structure absorbances were identified in this manner. Absorbances around 1648 cm^{-1} were assigned to aperiodic structure; absorbances around 1633 and 1625 cm^{-1} were assigned to β-strand. To provide quantitative assessment of the FTIR spectra, absorbance spectra were

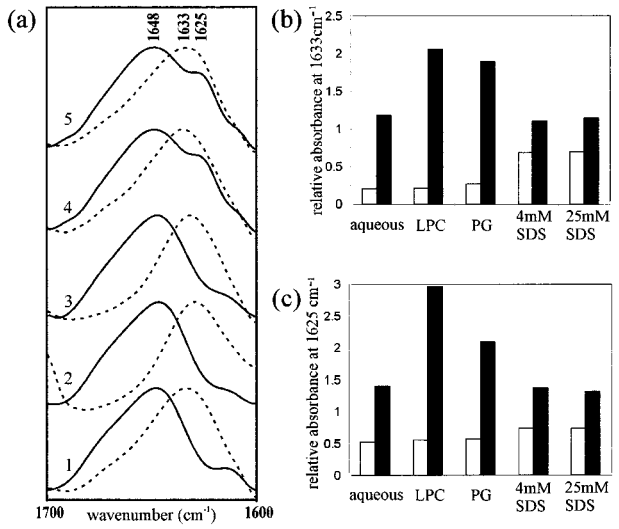

FIGURE 1: FTIR spectroscopy of wild-type $K_V3.4$ inactivation peptide. (a) Amide I regions of deconvolved spectra of reduced (solid line) and oxidized (dashed line) $K_V3.4$ inactivation peptide at 20 °C in (1) D_2O PBS (pD 7.4) and (2) cosolubilized with lysophosphatidylcholine micelles, (3) with phosphatidylglycerol vesicles, (4) with 4 mM sodium dodecyl sulfate, or (5) with 25 mM sodium dodecyl sulfate. (b) Comparison of the absorbance of infrared light at 1633 cm^{-1} relative to the absorbance at 1648 cm^{-1} of reduced (open bars) and oxidized (solid bars) forms of the $K_V3.4$ ball peptide in various environments. (c) Comparison of the absorbance of infrared light at 1625 cm^{-1} relative to the absorbance at 1648 cm^{-1} of reduced (open bars) and oxidized (solid bars) forms of the $K_V3.4$ ball peptide in various environments.

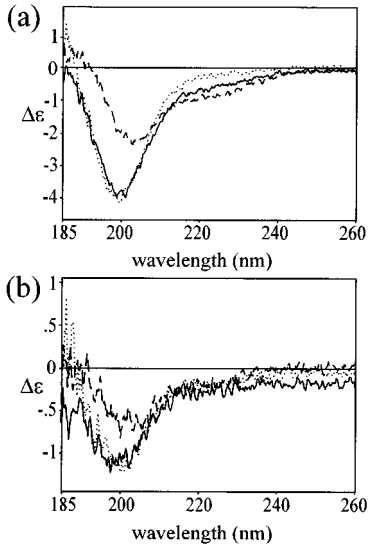

FIGURE 2: Far-UV CD spectroscopy of wild-type $K_V3.4$ inactivation peptide. (a) Far-UV CD spectra of reduced $K_V3.4$ inactivation peptide at 20 °C in 100 mM phosphate buffer (pH 7.4) (solid line), cosolubilized with lysophosphatidylcholine micelles (dotted line), or solubilized with 25 mM sodium dodecyl sulfate (dashed line). (b) Far-UV CD spectra of oxidized $K_V3.4$ inactivation peptide at 20 °C in 100 mM phosphate buffer (pH 7.4) (solid line), cosolubilized with lysophosphatidylcholine micelles (dotted line), solubilized with 25 mM sodium dodecyl sulfate (dashed line).

deconvolved and absorbance intensities at either of the β-structure wavenumbers were quantified relative to the absorbance intensity of the 1648 cm^{-1} aperiodic component in the same spectrum.

Relative amounts of secondary structure were assessed from CD spectra based on previous observations that aperiodic structures give strong negative bands around 200 nm whereas β-structures give strong positive bands at 200 nm (*20*, *21*). CD spectra of peptides containing aperiodic structures and β-structures therefore arise from a combination of these two features. Thus, for a given peptide the extent of adoption of β-structure can be assessed by the relative positivity of the 200 nm band; i.e., the more positive the 200 nm absorbance, the greater the extent of adoption of β-structure.

THREADER Modeling. The sequence of the $K_V3.4$ ball peptide was subjected to computerized structure prediction by the THREADER program (*16*). THREADER models protein structure by direct fitting of protein sequences onto the backbone coordinates of known protein structures. This backbone matching is performed in full three-dimensional space, incorporating specific pair interactions explicitly.

RESULTS

FTIR and CD Spectroscopy. (A) Wild-Type $K_V3.4$ Ball Peptide. Deconvolved infrared spectra of reduced and oxidized forms of wild-type $K_V3.4$ ball peptide in a range of environments are given in Figure 1a. Figure 1b,c represents these results in the form of bar charts in which absorbance intensities at 1633 and 1625 cm^{-1} wavenumbers (assignable to β-structures), respectively, for the peptide in different environments are compared to one another as a function of the absorbance intensity at 1648 cm^{-1} (assignable to aperiodic structures). The figures illustrate the extent to which the ball peptide adopts ordered β-structure under different conditions. Reduced $K_V3.4$ ball peptide in aqueous solution absorbs strongly around 1648 cm^{-1} in the amide I region of the infrared spectrum, characteristic of aperiodic structure. CD spectroscopy of reduced $K_V3.4$ ball peptide (Figure 2) shows a strong negative absorbance around 200 nm, again characteristic of aperiodic structure. This is consistent with recent NMR spectroscopic determination of the structure of the ball peptide in similar conditions (*13*) which indicated that the ball peptide adopted no classical backbone secondary structure characteristics; i.e., there was no presence of α-helix or β-strand, in aqueous solution under reducing conditions.

Lysophosphatidylcholine (LPC) is a zwitterionic lipid which forms micelles at ambient temperatures in aqueous buffer and which has previously been used to mimic the environment of the cell membrane in spectroscopic studies of membrane proteins (*22*). When cosolubilized with LPC micelles in order to recreate the conditions the ball peptide encounters when bound to the proposed hydrophobic inactivation binding site, the $K_V3.4$ ball peptide maintains the strong absorbance around 1648 cm^{-1} in the infrared spectrum characteristic of aperiodic structure. Similarly, the CD spectrum of the reduced $K_V3.4$ ball peptide cosolubilized with LPC contains the same strong negative absorbance observed for the ball peptide in aqueous solution. This indicates that interaction with a hydrophobic environment alone is not sufficient to evoke significant structural changes in the reduced $K_V3.4$ ball (Figures 1 and 2).

To mimic both the hydrophobicity of the inactivation ball binding pocket and the negative charge proposed to initially attract the ball to its binding site, the $K_V3.4$ ball peptide was cosolubilized in aqueous solution with vesicles of the anionic

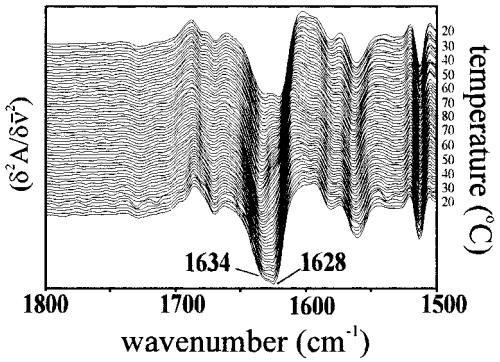

FIGURE 3: Temperature-resolved FTIR second-derivative spectra of oxidized wild-type K_V3.4 inactivation peptide in deuterated PBS (pD 7.4). The sample was heated from 20 to 80 °C and then cooled to 20 °C (heating then cooling run from bottom to top in the figure). Spectra shown are the result of 50 scans recorded every 2 °C and signal-averaged.

lipid phosphatidylglycerol (PG). CD spectroscopy of the ball peptide in this environment was not possible due to the light-scattering effects of the PG vesicles in solution. FTIR spectroscopy indicated, however, that in this negatively charged and hydrophobic environment the infrared absorbance of the ball peptide shifted away from 1648 cm^{-1} to a slightly lower wavenumber. This shift is apparent as a slight increase in the intensity of the 1633 and 1625 cm^{-1} β-strand components relative to the intensity of the 1648 cm^{-1} aperiodic component (Figure 1). This suggests that a partial adoption of β-structure by the K_V3.4 ball peptide occurred in these conditions. To further investigate this phenomenon, the reduced K_V3.4 ball peptide was solubilized in aqueous solution containing the anionic detergent sodium dodecyl sulfate (SDS) at both 4 mM and 25 mM, concentrations below and above the critical micellization concentration (CMC) of SDS, respectively. The intensities of bands at 1633 and 1625 cm^{-1}, assignable to β-structure, were increased by solubilization of the ball peptide in either 4 mM or 25 mM detergent (Figure 1). CD spectra showed reduced negativity in the 200 nm band associated with aperiodic structures upon solubilization with SDS (Figure 2a). This is probably due to the positive absorbance at 200 nm of β-structures in the peptide when solubilized in SDS. Both FTIR and CD spectroscopy indicate that the reduced K_V3.4 ball peptide adopts β-structure to a greater extent in anionic detergent than in aqueous or nonionic conditions.

The effects of intramolecular linkage of Cys^6 and Cys^{24} (i.e., "cyclisation") on the structure of the K_V3.4 ball peptide and its ability to adopt β-structure in different environments were investigated using oxidized ball peptide. In contrast to the reduced (noncyclic) form of the K_V3.4 ball peptide, the oxidized (cyclic) K_V3.4 ball peptide is capable of adopting elements of β-structure in aqueous solution in the absence of lipid or detergent. This is evident from the shift of the main infrared absorbance peak from 1648 cm^{-1} (aperiodic structure) in reducing conditions to around 1633 cm^{-1} (β-structure) in oxidizing conditions (Figure 1). The β-structure adopted by the ball peptide in oxidizing conditions in aqueous solution is highly thermostable, showing only a slight shift upward in FTIR absorbance wavenumber upon heating from 20 to 80 °C, which is reversible upon cooling back down to 20 °C (Figure 3). This shift is indicative of a reversible heat-induced reduction of hydrogen-bonding strength between β-strands (*19*, *23*). The shift to absorbance of infrared light at lower wavenumbers, characteristic of an increase in β-structures, by the cyclic K_V3.4 ball peptide is more marked when cosolubilized with anionic lipid (the 1625 cm^{-1} absorbance is twice the intensity of the 1648 cm^{-1} absorbance in phosphatidylglycerol in this case) or detergent. The most dramatic shift is observed for the cyclic ball peptide with LPC micelles, which gives a 1625 cm^{-1} absorbance 3 times the intensity of the 1648 cm^{-1} absorbance (Figure 1). FTIR spectroscopy of the cyclic ball peptide in aqueous solution with SDS indicated no significant differences between the extent of adoption of β-structure in 25 mM SDS compared to in the less concentrated, nonmicellar 4 mM SDS. CD spectroscopy results showed that the negativity of the 200 nm band associated with aperiodic structures was lower with the cyclic peptide than with the reduced peptide under similar conditions (−1 compared to −4, respectively, when the peptide was solubilized with 25 mM SDS; Figure 2b). Both FTIR and CD spectroscopy results showed that in all environments studied the cyclic K_V3.4 ball peptide adopts a greater proportion of β-structure than the noncyclic K_V3.4 ball peptide does in similar conditions (Figures 1 and 2).

(B) V7E Mutant Ball Peptide. In contrast to the wild-type K_V3.4 ball peptide, the V7E mutant ball peptide was incapable of adopting elements of β-structure, regardless of environment or oxidation state. This is illustrated in Figure 4a which shows that the infrared absorbance of the mutant peptide remains centered around 1648 cm^{-1} in all conditions, in significant contrast to the marked shift to lower wavenumbers observed upon oxidation of the wild-type ball peptide (Figure 1a). Figure 4b,c shows that the absorbances at 1633 and 1625 cm^{-1} (assignable to β-structure) are similar in reduced and oxidized V7E ball peptides, and remain relatively low (0.1−0.7, compared to a maximum of 3 in the wild-type ball peptide) when compared to the absorbance at 1648 cm^{-1}. Figure 4d,e highlights the inability of the mutant ball peptide to adopt β-structure by comparing the relatively large intensities of the 1625 and 1633 cm^{-1} (β-structure) absorbances of the wild-type ball peptide to the much lower intensities of these β-structure absorbances observed for the mutant ball peptide.

Structure Prediction Based on Amino Acid Sequence. THREADER modeling of the structure of the K_V3.4 ball peptide gave a consensus structure consisting of two regions of extended conformation linked halfway along the sequence of the ball peptide by a region of coil or turn. The consensus structure and top 10 pairwise hits are illustrated in Figure 5. The consensus fraction cutoff in this secondary structure comparison was 0.65, and the strongest pairwise energy score was −2.73. The results suggest that the ball peptide has a propensity to adopt, in certain conditions, a hairpin structure with hydrogen-bonding occurring to some extent between the two strands of the hairpin. The appearance of helix in the 2nd, 3rd, and 5th entries in the sorted list may indicate that the strand curls around or frays at the end, with a lack of H-bonding to the other strand in this region.

DISCUSSION

The spectroscopic results indicate that the oxidized (cyclic) K_V3.4 ball peptide adopts a conformation containing a larger

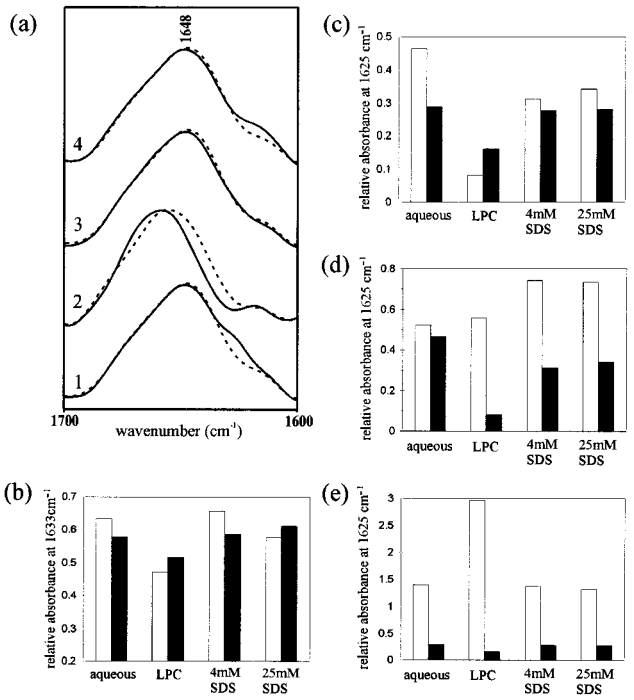

FIGURE 4: FTIR spectroscopy of V7E mutant inactivation peptide. (a) Amide I regions of deconvolved spectra of reduced (solid line) and oxidized (dashed line) V7E mutant inactivation peptide at 20 °C in (1), D_2O PBS (pD 7.4) and (2) cosolubilized with lysophosphatidylcholine micelles, (3) with 4 mM sodium dodecyl sulfate, or (4) with 25 mM sodium dodecyl sulfate. (b) Comparison of the absorbance of infrared light at 1633 cm^{-1} relative to the absorbance at 1648 cm^{-1} of reduced (open bars) and oxidized (solid bars) forms of the V7E mutant ball peptide in various environments. (c) Comparison of the absorbance of infrared light at 1625 cm^{-1} relative to the absorbance at 1648 cm^{-1} of reduced (open bars) and oxidized (solid bars) forms of the V7E mutant ball peptide in various environments. (d) Comparison of the absorbance of infrared light at 1625 cm^{-1} relative to the absorbance at 1648 cm^{-1} of wild-type (open bars) and V7E mutant (solid bars) forms of reduced $K_V3.4$ ball peptide in various environments. (e) Comparison of the absorbance of infrared light at 1625 cm^{-1} relative to the absorbance at 1648 cm^{-1} of wild-type (open bars) and V7E mutant (solid bars) forms of oxidized $K_V3.4$ ball peptide in various environments.

```
                      10        20
sequence   MISSVCVSSYRGRKSGNKPPSKTCLKEE
concensus  EEE EEEEEEE CCCCC EEEEEEE  C

1hjrA0     EEECEEEEEEEEECCEEEEEEEEEECC
1shp00     EEECEEEEEECCCCCCCCCHHHHHHHH
5pti00     EEECEEEEEECCCCCCCCCHHHHHHH
2polA0     EEECEEEEEC------CEEEEEEEECC
1dem00     EEECEEEEEECCCCCCCCCHHHHHHH
2rmcA0     EEEEEEEEEEEC-CEEEEEEEEECC
1scs00     EEEEEEEEEEECCCCCEEEEEEEECC
1ifc00     EECCEEEEEEEC----CEEEEEEEEC
1gecE0     EEEEEEEEEEC-----CEEEEEEECC
1tetH1     CCCEEEEEEEC---CCEEEEEEECC
```

FIGURE 5: THREADER prediction of the structure of wild-type $K_V3.4$ inactivation peptide. The top 10 hits based on pairwise interactions are listed with their corresponding secondary structures, aligned below the sequence of the $K_V3.4$ ball peptide and its consensus structure based on the top hits. Structure abbreviations: C = coil or aperiodic, E = extended (β-structure), H = α-helix. Boldface type indicates consensus structure and extent of agreement with this consensus in the top 10 hits.

proportion of ordered β-structure than the reduced (noncyclic) $K_V3.4$ ball peptide in a similar environment (Figure 1). The reduced $K_V3.4$ ball peptide adopts a greater amount of ordered β-structure in hydrophobic, negatively charged environments than in aqueous solution or when cosolubilized with zwitterionic lipid. The oxidized $K_V3.4$ ball peptide, however, adopts a maximal proportion of β-structure in the zwitterionic lipid LPC, and the presence of negative charge reduces this ability to adopt β-structure. Substitution of the hydrophobic valine residue at position 7 for a negatively charged glutamate residue ablates the ability of the ball peptide to adopt ordered β-structure, regardless of oxidation state or solubilization in zwitterionic or anionic lipids or detergents (Figure 4).

Previous spectroscopic studies on the *Shaker* B inactivation ball peptide in anionic lipid environments (*24*) have indicated similar structural trends to those observed for the noncyclic $K_V3.4$ inactivation ball peptide in the current study. However, the noncyclic $K_V3.4$ inactivation ball peptide is able to adopt a degree of β-sheet in anionic detergent (SDS) below the CMC of this detergent, whereas the *Shaker* B ball peptide requires micelles of the anionic detergent sodium cholate to attain a partial β-sheet structure. This may indicate that the two ball peptides (from $K_V3.4$ and from *Shaker* B) have slightly different requirements for the attainment of β-structure, and the inability of the *Shaker* B ball to attain β-structure in nonmicellar, anionic detergent may be due to its lack of stable structure in aqueous solution (compare with the $K_V3.4$ ball peptide which adopts a more rigid hairpin-like conformation in aqueous solution). In the *Shaker* B study, it is postulated that the inactivation peptide adopts β-structures upon exposure to negatively charged residues, giving it the charge balance necessary for insertion into a hydrophobic binding pocket to facilitate channel inactivation. Our results combined with those in the recent NMR study of the $K_V3.4$ inactivation ball peptide (*13*) indicate that the noncyclic $K_V3.4$ ball peptide adopts a rigid, convoluted hairpin-like structure in aqueous solution. Our results demonstrate that exposure to a negatively charged, hydrophobic environment equivalent to that encountered by the ball peptide during channel inactivation alters the conformation of the $K_V3.4$ ball peptide such that a partial β-structure is adopted. In their NMR study (*13*), Antz and co-workers state that analysis of the chemical shifts in the different states of the $K_V3.4$ ball peptide shows that formation of a disulfide bond between Cys^6 and Cys^{24} causes structural changes only in the vicinity of the two cysteines. The most likely explanation for the β-structures detected spectroscopically in the $K_V3.4$ ball peptide in the current study after oxidation of the ball peptide or exposure to an anionic and hydrophobic environment, therefore, is the formation of intramolecular interstrand hydrogen bonds characteristic of β-sheet between residues surrounding Cys^6 and residues surrounding Cys^{24}. This equates to adoption of a partial β-hairpin structure by the $K_V3.4$ ball peptide under certain conditions (Figure 6). This is consistent with the partial β-hairpin predicted by the THREADER program. Our results indicate that the cyclic version of the $K_V3.4$ ball peptide has a higher propensity to form this partial β-hairpin than does the noncyclic $K_V3.4$ ball peptide. The suggestion based on THREADER results that fraying occurs at the ends of the hairpin is consistent with the three-dimensional structure of the reduced ball peptide in aqueous solution as determined by NMR spectroscopy (*13*).

In conclusion, we have demonstrated that although the noncyclic $K_V3.4$ ball peptide adopts a different structure in

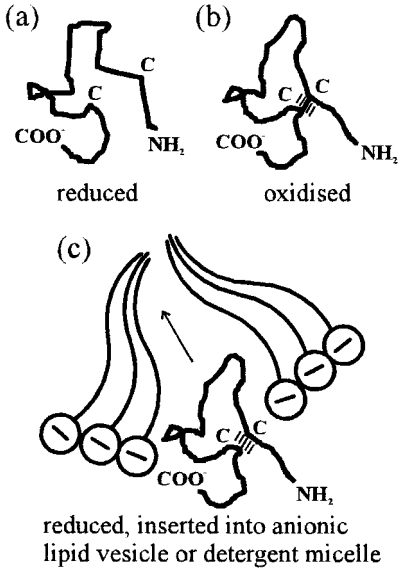

FIGURE 6: Model of conformational changes undergone by wild-type K_V3.4 inactivation peptide. (a) Convoluted hairpin-like structure of the K_V3.4 inactivation peptide in aqueous solution under reducing conditions, shown as the backbone structure of the peptide determined by NMR spectroscopy (*13*). (b) When the K_V3.4 ball peptide is oxidized, interstrand intramolecular hydrogen bonding characteristic of β-sheet (represented by thin lines between the two strands of the hairpin) forms concomitantly with formation of a disulfide bond (represented by a thick line between the two strands of the hairpin) between Cys^6 and Cys^{24}. (c) In a negatively charged, hydrophobic environment, interstrand intramolecular hydrogen bonding characteristic of β-sheet is attained by the K_V3.4 inactivation ball peptide without the necessity of disulfide bond formation.

aqueous solution than that of the *Shaker* B ball peptide, the noncyclic K_V3.4 ball displays an ability similar to that of the *Shaker* B ball peptide for the partial adoption of β-sheet when exposed to an environment mimicking that of the inactivation binding site. From previous studies, it has been concluded that the ability to adopt β-structure is essential to the inactivation capabilities of the *Shaker* B ball peptide (*24*). Furthermore, investigators have previously suggested that in vivo oxidation of cysteines in the K_V3.4 inactivation ball domain may be possible, and have demonstrated that Cys^{13} and Cys^6 of the K_V1.4 and K_V3.4 ball peptides, respectively, can be linked by a disulfide bond to a cysteine on the main body of the channel by in vitro oxidation. This suggests a regulatory role for N-terminal cysteine residues whereby locally oxidizing conditions can lead to immobilization of the inactivation ball domain and consequent prevention of channel inactivation (*8*). Based on these proposals, together with our observation that oxidative cyclization of the K_V3.4 ball peptide increases its propensity to form the postulated channel-inactivating (partial β-hairpin) conformation, we propose that an alternative K_V channel regulatory step may occur via cyclization of the K_V3.4 ball peptide by formation of a disulfide linkage between Cys^6 and Cys^{24}, inducing an optimal conformation for channel inactivation and thereby favoring the inactivated state by increasing the tendency of the K_V3.4 ball peptide to bind to its channel inactivation site. This is one mechanism by which the gating kinetics of the mammalian K_V channel may be fine-tuned by the oxidative state of its immediate environment.

ACKNOWLEDGMENT

We thank Dr. Guiliano Siligardi at the National Chiroptical Spectroscopy Facility (EPSRC), King's College, Manresa Road, London, for assistance with the circular dichroism measurements.

REFERENCES

1. Hoshi, T., Zagotta, W. N., and Aldrich, R. W. (1990) *Science 250*, 533−538.
2. Zagotta, W. N., Hoshi, T., and Aldrich, R. W. (1990) *Science 250*, 568−571.
3. Isacoff, E. Y., Jan, Y. N., and Jan, L. Y. (1991) *Nature 353*, 86−90.
4. Murrell-Lagnado, R. D., and Aldrich, R. W. (1993a) *J. Gen. Physiol. 102*, 949−975.
5. Murrel-Lagnado, R. D., and Aldrich, R. W. (1993b) *J. Gen. Physiol. 102*, 977−1003.
6. Jan, L. Y., and Jan, Y. N. (1992) *Cell 69*, 715−718.
7. Durrel, S. R., and Guy, H. R. (1992) *Biophys. J. 62 (Discussions)*, 238−250.
8. Ruppersberg, J. P., Stocker, M., Pongs, O., Heinemann, S. H., Frank, R., and Koenen, M. (1991) *Nature 352*, 711−714.
9. Schroter, K.-H., Ruppersberg, J. P., Wunder, F., Rettig, J., Stocker, M., and Pongs, O. (1991) *FEBS Lett. 278* (2), 211−216.
10. Rettig, J., Wunder, F., Stocker, M., Lichtinghagen, R., Mastiaux, F., Beckh, S., Kues, W., Pedarzani, P., Schroeter, K. H., and Ruppersberg, J. P. (1992) *EMBO J. 11*, 2473−2486.
11. Stephens, G. J., and Robertson, B. (1995) *J. Physiol. 102*, 1057−1083.
12. Stephens, G. J., Owen, D. G., Opalko, A., and Robertson, B. (1996) *J. Physiol. 496 (1)*, 145−154.
13. Antz, C., Geyer, M., Fakler, B., Schott, M. K., Guy, H. R., Frank, R., Ruppersberg, J. P., and Kalbitzer, H. R. (1997) *Nature 385*, 272−274.
14. Surewicz, W. K., and Mantsch, H. H. (1988) *Biochim. Biophys. Acta 952*, 115−130.
15. Braiman, M. S., and Rothschild, K. J. (1988) *Annu. Rev. Biophys. Biophys. Chem. 17*, 541−570.
16. Jones, D. T., Taylor, W. R., and Thornton, J. M. (1992) *Nature 358*, 86−89.
17. Carpino, L. A., and Han, G. Y. (1992) *J. Org. Chem. 37*, 3404−3409.
18. Merrifield, R. B. (1963) *J. Am. Chem. Soc. 85*, 2149−2154.
19. Jackson, M., and Mantsch, H. H. (1995) *Crit. Rev. Biochem. Mol. Biol. 30* (2), 95−120.
20. Johnson, W. C., Jr. (1990) *Proteins: Struct., Funct., Genet. 7*, 205−214.
21. Venyaminov, S. Y., Baikalov, I. A., Wu, C. S. C., and Jen, T.-Y. (1991) *Anal. Biochem. 198* (2), 250−255.
22. Haris, P. I., Ramesh, B., Brazier, S., and Chapman, D. (1994a) *FEBS Letts. 349*, 371−374.
23. Surewicz, W. K., Mantsch, H. H., and Chapman, D. (1993) *Biochemistry 32*, 389−394.
24. Fernandez-Ballester, G., Gavilanes, F., Albar, J. P., Criado, M., and Ferragut, J. A. (1995) *Biophys. J. 68*, 858−865.

BI972350C